

Surrogate Modeling of Stochastic Dynamical Systems

Aditya Sai¹ and Nan Kong¹

Abstract—Dynamical, or time-varying, systems describe a variety of phenomena found within many branches of science and engineering. Certain dynamical systems may be unwieldy to simulate repetitively, especially if the model contains uncertainty in the form of stochastic terms and must account for a global range of model behavior. Surrogate modeling using sparse grid interpolation can alleviate the burden associated with increasing dimension of the parameter space. Previous stochastic differential equation (SDE)-based sparse grid approaches have not presented a comprehensive analysis on the benefits of tuning sparse grid settings. This letter seeks to explore such settings, including the resolution level and the dimensional adaptivity of the sparse grid. Results suggest that the number of support nodes and the degree of dimensional adaptivity can be strategically tuned to construct an accurate, efficient interpolant.

Index Terms—surrogate modeling, dynamical system, Itô stochastic differential equation, sparse grid interpolation, systems biology

I. INTRODUCTION

Dynamical systems enable modeling of time-varying real-world systems. The underlying models can be described by differential equations, where each equation describes the rate of change of a single state variable as a function of model parameters, time and other state variables, and can be solved numerically using discretized approximations to the true solution. Most mechanistic and semi-mechanistic mathematical models of dynamical systems are developed using ordinary differential equations. Nevertheless, random external disturbances are known to influence such systems, necessitating the need to model them with stochastic processes [1]. Here, we focus on Itô stochastic differential equations (SDEs):

$$\mathbf{X}(t) = f(\mathbf{X}, t, \boldsymbol{\theta})dt + g(\mathbf{X}, t, \boldsymbol{\theta})d\mathbf{B}(t) \quad \mathbf{X}(0) = \mathbf{X}_0, \quad (1)$$

where $\mathbf{X} \in \mathbb{R}^N$ is a continuous time stochastic process, $\mathbf{B} \in \mathbb{R}^M$ is a Brownian motion process, t is time, $\boldsymbol{\theta} \in \mathbb{R}^P$ are model parameters, $f(\cdot) : \mathbb{R}^N \times [0, T] \times \Theta \rightarrow \mathbb{R}^N$ is the drift term (deterministic component), and $g(\cdot) : \mathbb{R}^N \times [0, T] \times \Theta \rightarrow \mathbb{R}^{N \times M}$ is the diffusion term (stochastic component).

Complex dynamical systems are often difficult to simulate when considering a large number of model parameters [2]–[4]. Furthermore, local searches of the pertinent factors may be insufficient to characterize the wide range of possible behaviors exhibited by the system in question. Sparse grids allow for global, computationally efficient exploration of the parameter space using tensor-product quadrature [5]–[7]. Sparse grid interpolants mitigate the curse of dimensionality

associated with higher dimensional parameter spaces by sampling the parameter space strategically and evaluating the original model sparsely. The resulting surrogate model can be used in model-based control and optimization without sacrificing modeling accuracy or performing unnecessary model evaluations. The concept of sparse grid interpolation, and surrogate modeling in general, is not unlike that of compressive sensing, where a compressible signal is recovered from a limited number of measurements [8]. Fig. 1 demonstrates the application of sparse grid interpolation to a simple 3-dimensional trigonometric function.

In the stochastic domain, sparse grids have been applied to stochastic partial differential equations with random inputs [9]–[14], backwards stochastic differential equations with random inputs [15], and differential algebraic equations with random parameters [16]. SDEs with white noise were also explored with the sparse grid method [17], with the intent of determining the optimal time step and noise level for first-order convergence of the method. When the integration and discretization step sizes were varied, the increase in the number of random variables along the stochastic process led to an increase in the number of points needed to construct the sparse grid, which we refer to as support nodes.

While stochastic models have found widespread usage in finance [18], [19], the models we explore in this paper were found in the systems biology literature. Systems biology is concerned with the systems level representation of biological phenomena [20]. Examples of SDE-based models in systems biology include: (1) the human nervous system [21]–[23], (2) a glucose regulatory system for type 1 diabetes patients [24], (3) the JAK-STAT signaling pathway [25], (4) the euglycemic hyperinsulinemic clamp [26], and (5) predator-prey dynamics in polluted environments [27]. There is a need to accurately model these biological phenomena and their inherent variability.

In this work, we perform a comparative study of two stochastic dynamical systems to understand how certain features of the sparse grid can be tuned to improve the accuracy of the resulting surrogate model. The surrogate model estimates the mean and variance of an ensemble of SDE trajectories simulated across various points in the parameter space. After reviewing sparse grid interpolation, we present results related to modifying certain features of the sparse grid, such as the number of support nodes used to construct the interpolant. Our results reveal that while these features may all contribute to improving interpolant accuracy, they do so disproportionately. We then summarize our work and suggest future extensions.

Manuscript received July 20, 2017; revised October 11, 2017.

¹The authors are with the Weldon School of Biomedical Engineering, Purdue University, West Lafayette, Indiana, USA (email: asai@purdue.edu; nkong@purdue.edu)

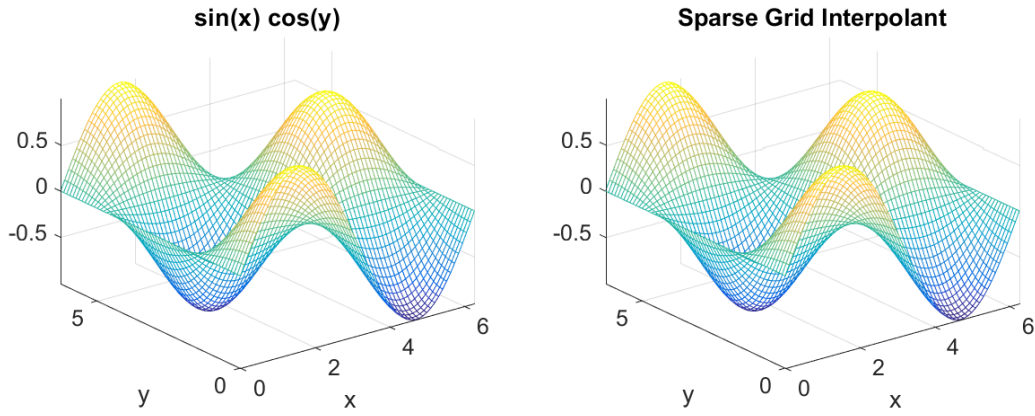


Fig. 1. Function $f = \sin x \cos y$ evaluated on a grid $[0, 2\pi] \times [0, 2\pi]$ using both the original function (left) and the sparse grid interpolant (right). The interpolant was produced with a relative error of 0.44%, absolute error of 0.0087, and 321 support nodes.

II. SPARSE GRID INTERPOLATION

In sparse grid interpolation, the support nodes are selected in a predefined manner; a nested, hierarchical sampling scheme [6], [7], [28] recycles nodes from lower levels of resolution to use in higher levels.

A mathematical formulation of sparse grids now follows from [5]–[7], [29]–[31]. Consider a function $f : [0, 1]^d \rightarrow \mathbb{R}$ that is to be interpolated on a finite number of support nodes. Dimensions that are not of unit length can be rescaled. Here, f represents the sample average and standard deviation of multiple SDE trajectories sampled at discrete time points. For a given f , a univariate interpolation function can be constructed:

$$\mathcal{U}^i(f) = \sum_{j=1}^{m_i} a_j^i \cdot f(x_j^i) \quad (2)$$

where $i \in \mathbb{N}$, $a_j^i \in C([0, 1])$, $a_j^i(x_j^i) = \delta_{jl}$, $l \in \mathbb{N}$ are the univariate basis functions, $x_j^i \in X_i = \{x_1^i, \dots, x_{m_i}^i\}$, $x_j^i \in [0, 1]$, $1 \leq j \leq m_i$, are the support nodes.

Extending this interpolation function to multiple dimensions, the multivariate formula, using the full tensor product formulation, is:

$$(\mathcal{U}^{i_1} \otimes \dots \otimes \mathcal{U}^{i_d})(f) = \sum_{j_1=1}^{m_{i_1}} \dots \sum_{j_d=1}^{m_{i_d}} (a_{j_1}^{i_1} \otimes \dots \otimes a_{j_d}^{i_d}) f(x_{j_1}^{i_1}, \dots, x_{j_d}^{i_d}). \quad (3)$$

The number of support nodes required for the full tensor product representation is $\prod_{j=1}^d m_{i_j}$, which is computationally intractable for high dimensions d .

The Smolyak construction aims to substantially decrease the number of support nodes used while preserving the interpolation properties observed in the 1-dimensional case. Define the difference function $\Delta^i = \mathcal{U}^i - \mathcal{U}^{i-1}$, $\mathcal{U}^0 = 0$ and multi-index $\mathbf{i} \in \mathbb{N}^d$, $|\mathbf{i}| = i_1 + \dots + i_d$. Now, define the Smolyak interpolant as:

$$A_{n+d,d}(f) = \sum_{k=0}^n \sum_{|\mathbf{i}|=k+d} (\Delta^{i_1} \otimes \dots \otimes \Delta^{i_d})(f). \quad (4)$$

The inner sum can be expressed as

$$\sum_{|\mathbf{i}|=k+d} \sum_j (a_{j_1}^{i_1} \otimes \dots \otimes a_{j_d}^{i_d})(f(\mathbf{x}_j^{\mathbf{i}}) - A_{k+d-1,d}(f(\mathbf{x}_j^{\mathbf{i}}))), \quad (5)$$

where \mathbf{j} is the multi-index (j_1, \dots, j_d) , $j_l = 1, \dots, m_{i_l}^{\Delta}$, $l = 1, \dots, d$, and the nodes $\mathbf{x}_j^{\mathbf{i}} = (x_{j_1}^{i_1}, \dots, x_{j_d}^{i_d})$, $x_{j_l}^{i_l}$ is the j_l th element of $X_{\Delta}^{i_l} = X^{i_l} \setminus X^{i_l-1}$, $X^0 = \emptyset$, and $m_{i_l}^{\Delta} = |X_{\Delta}^{i_l}|$. The support nodes can be chosen in an hierarchical fashion such that $X^i \subset X^{i+1}$, $i \in \{i_1, \dots, i_d\}$.

It is also useful to compute the absolute (E_{abs}^n) and relative (E_{rel}^n) errors of the Smolyak interpolant using correction terms known as hierarchical surpluses ($w_j^{k,\mathbf{i}}$):

$$w_j^{k,\mathbf{i}} = f(\mathbf{x}_j^{\mathbf{i}}) - A_{k+d-1,d}(f(\mathbf{x}_j^{\mathbf{i}})), \quad (6)$$

$$E_{abs}^n = \max_{\mathbf{i}, \mathbf{j}} w_j^{n,\mathbf{i}}, \quad (7)$$

$$E_{rel}^n = \frac{\max_{\mathbf{i}, \mathbf{j}} w_j^{n,\mathbf{i}}}{\max_{\mathbf{i}, \mathbf{j}} f(\mathbf{x}_j^{\mathbf{i}}) - \min_{\mathbf{i}, \mathbf{j}} f(\mathbf{x}_j^{\mathbf{i}})}. \quad (8)$$

The conventional sparse grid fails to consider the impact errors can have on the quality of the interpolant produced. Adaptive sparse grids [5] build on the conventional formulation by using generalized error indicators that consider the influence of the error in comparison to the necessary computational work:

$$g_{\mathbf{j}} = \max \left\{ w \frac{|\Delta^{\mathbf{j}} f|}{|\Delta^{\mathbf{1}} f|}, (1-w) \frac{n_{\mathbf{1}}}{n_{\mathbf{j}}} \right\}, \quad (9)$$

where $w \in [0, 1]$ is a weight for the error indicator $g_{\mathbf{j}}$, $n_{\mathbf{k}}$ is the number of function evaluations for an index set \mathbf{k} . Conventional sparse grids are formed when $w = 0$, and only the number of function evaluations are considered. When $w = 1$, the error indicators will decay with increasing indices. Intermediate values of w compromise between excessive work and high error.

The approximation properties of the sparse grid rely on basis functions to select the required support nodes. Chebyshev-based node distributions can be used for higher-order polynomial interpolation, where the function to be interpolated is smooth and higher accuracy is required [32]. In this work, we use Chebyshev-Gauss-Lobatto nodes [30], which are defined as follows:

$$m_i = \begin{cases} 1, & i = 1 \\ 2^{i-1} + 1, & i > 1 \end{cases} \quad (10)$$

$$x_j^i = \begin{cases} -\cos \frac{\pi \cdot (j-1)}{m_i-1}, & m_i > 1 \\ 0, & m_i = 1. \end{cases} \quad (11)$$

For implementation purposes, Matlab was used as the simulation environment for the models discussed here. The Euler-Maruyama method, a first-order stochastic Taylor expansion, was used to integrate SDEs [33]–[35]:

$$\mathbf{X}(t_{q+1}) = \mathbf{X}(t_q) + f(\mathbf{X}(t_q), q\delta t, \boldsymbol{\theta})\delta t + g(\mathbf{X}(t_q), q\delta t, \boldsymbol{\theta})(B(t_q) - B(t_{q-1})), \quad (12)$$

where δt is the integration time step, and $q = 0, \dots, T/\delta t$. Sparse grid interpolation was performed using the Sparse Grid Interpolation Toolbox [32].

III. RESULTS

We examine two SDE-based models: a dynamic contrast enhanced imaging (DCEI) model used in monitoring the efficacy of cancer therapeutics [1], and a predator-prey (PP) model commonly found in ecology [36]. We compare results for 3-dimensional (3D, DCEI and PP), 7-dimensional (7D, DCEI only), and 8-dimensional (8D, PP only) interpolants. The dimensionality of the interpolant is the number of parameters that were varied and explored by the interpolant.

A. Simulation Conditions and Convergence Error

Each model had to be tuned for compatibility with sparse grid interpolation by choosing both the simulation conditions and the number of realizations. Simulation conditions for the model, such as initial conditions, durations of the simulation, desired model states, and parameters to explore in the parameter space, were determined first. These conditions were defined in large part to conform with the scope of the overall study and are presented in the Appendix. The ranges of the parameter space were chosen by perturbing the nominal value of each parameter by 10%. Once the simulation conditions were defined, the number of realizations for each model had to be determined to capture the stochasticity present in the models.

We used a convergence error (CE) metric to quantify the difference between model states with successive number of realizations, which is defined in the Appendix. The CE metric is computed across all support nodes in the parameter space used to construct the sparse grid. We then increase the number of realizations incrementally by 10, until the mean CE is less than some threshold ϵ , which we set to 10^{-3} . 20 realizations were sufficient to achieve this threshold for both models, as mean CE values of $9.2 \cdot 10^{-6}$ and $3.3 \cdot 10^{-4}$ were found for the DCEI and PP models, respectively.

B. Interpolation Depth

The interpolation depth is a measure of the resolution of the sparse grid; specifically, it is the degree of the polynomial, which the univariate interpolation function can exactly match [5], [30]. A conventional sparse grid can undergo a series of symmetric subdivisions in order to sample

the parameter space more finely and systematically. We first explore interpolation depth on a conventional sparse grid to observe whether this basic feature provides significant error reduction as it is increased. Fig. 2 shows the relative error and the number of support nodes needed as the depth is increased for both 3D and 7D interpolants with the DCEI model. As expected, the 7D interpolant requires more support nodes to provide a comparable level of accuracy to the 3D interpolant. A monotonic relationship exists between the number of support nodes and the relative error; more accuracy requires more samples.

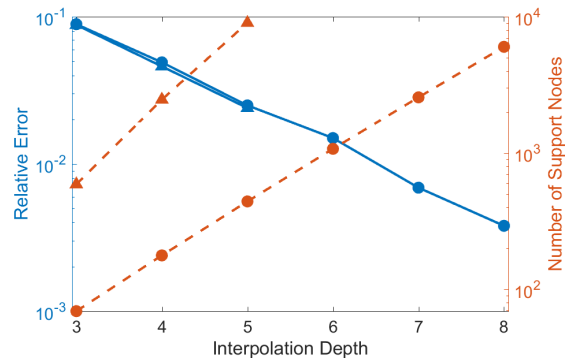


Fig. 2. Relative error and number of support nodes as a function of the interpolation depth for the DCEI model. Blue lines with circles (triangles) correspond to relative errors of the 3D (7D) interpolant. Orange dashed lines with circles (triangles) correspond to number of support nodes with 3D (7D) interpolant.

C. Dimensional Adaptivity

While increasing the depth of the interpolant will allow more support nodes to be systematically sampled and evaluated, it comes at an increased cost. Adaptivity provides an opportunity to tailor sampling and evaluation of support nodes to each individual model. Adaptive sparse grids allow for improvements in the accuracy of the interpolant to be made in the regions of the parameter space where it is needed most. The degree of dimensional adaptivity indicates the tendency of the underlying algorithm to sample adaptively. A greedy, adaptive approach will tend to sample points in the dimension that presents the greatest potential in error reduction, while a conservative, standard approach will ensure a conventional sparse grid is constructed [5]. The degree-balancing approach to dimensional adaptivity allows for gradual replacement of conventionally sampled support nodes by adaptively sampled ones as the degree of adaptivity is increased [32]. The degree of adaptivity was varied to assess its influence on interpolant accuracy with respect to the PP model.

Fig. 3 shows the relative error and the number of support nodes sampled as the degree of adaptivity is increased. The number of support nodes decreased steadily for both interpolants. The relative error also decreased significantly as adaptivity was increasingly employed. Fewer support nodes are required as adaptivity predominates, suggesting that sampling support nodes asymmetrically with respect to the parameter space is useful and essential for error reduction. In contrast with interpolation depth, moving towards more accurate interpolants does not necessarily require more samples. In fact, the fully adaptive interpolant demands fewer

support nodes than its non-adaptive counterpart, regardless of dimensionality.

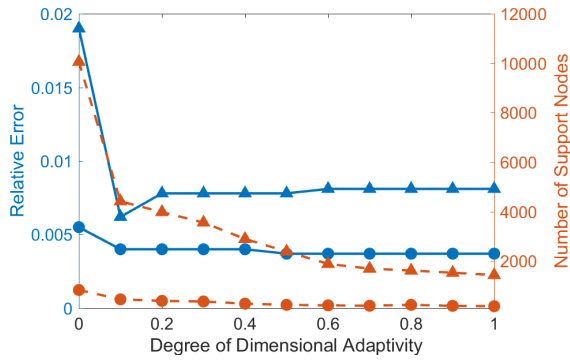


Fig. 3. Relative error and number of support nodes as a function of degree of dimensional adaptivity for the PP model. Blue lines with circles (triangles) correspond to relative errors of 3D (8D) interpolant. Orange dashed lines with circles (triangles) correspond to number of support nodes with 3D (8D) interpolant.

D. Number of Support Nodes

Having shown that an adaptive interpolant can reduce the error of the interpolant more than the interpolation depth, we proceed a step further by examining the effect of changing the number of support nodes. Specifically, we study how imposing caps on the number of support nodes influences accuracy for a fully adaptive interpolant. Fig. 4 illustrates that the 3D interpolant obtains a relative error almost two orders of magnitude lower than the 8D version. The 3D interpolant has achieved an error of less than 10^{-3} with less than 1,000 nodes. However, the 8D interpolant can be constructed with low error as well, settling near 10^{-3} when 10,000 nodes are used. With a sufficient number of nodes, a suitable error can be achieved for models with higher dimensionality.

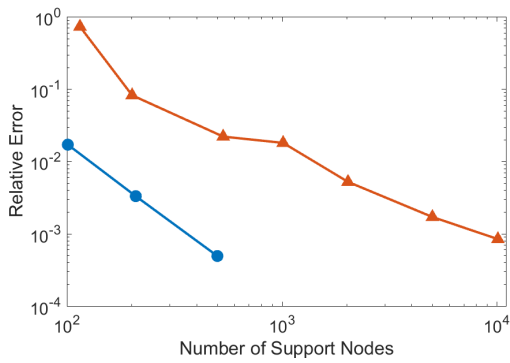


Fig. 4. Relative error as a function of the support nodes for the PP model with a fully adaptive sparse grid. The blue line with circles represent values obtained from a 3D interpolant, while the orange line with triangles indicate values obtained from an 8D interpolant.

IV. CONCLUSION

With surrogate models, researchers can fully study the spectrum of possible hypotheses coded by different model parameter values, without having to directly integrate the underlying model, which is often computationally prohibitive. The approach discussed here interpolates the first two statistical moments of an ensemble of SDE trajectories simulated

at each support node. It does so by analyzing a variety of computational factors that influence the accuracy of the solution, in order to suggest possible configurations that produce superior interpolants. Results suggest that the interpolation depth may confer fewer advantages in accuracy per point sampled, compared to the degree of dimensional adaptivity; more model evaluations do not necessarily translate to a more accurate surrogate model. Future work will attempt to sample multiple realizations of the SDE solver at each support node adaptively. This letter serves as an exploration of the true stochastic dynamics of SDE models using computationally expedient surrogate modeling.

APPENDIX

A. Dynamic Contrast Enhanced Imaging (DCEI) Model

$$[Q_P(0), Q_I(0)] = [0, 0] \quad (13)$$

$$dQ_P = \left(\frac{F_T V_B - PS}{V_B(1-h)} Q_P + \frac{PS}{V_e} Q_I - \frac{F_T}{V_B(1-h)} Q_P \right) dt + \sigma_1 dB_1 \quad (14)$$

$$dQ_I = \left(\frac{PS}{V_B(1-h)} Q_P - \frac{PS}{V_e} Q_I \right) dt + \sigma_2 dB_2 \quad (15)$$

where Q_P (Q_I) is the quantity of contrast agent in the blood plasma (interstitial space), F_T is the blood perfusion flow, h is the hematocrit fraction, PS is the permeability surface area product of tissue, and V_b (V_e) is the blood (extracellular) volume. σ_1 and σ_2 are the intensities of the noise processes.

TABLE I
SIMULATION CONDITIONS FOR DYNAMIC CONTRAST ENHANCED IMAGING (DCEI) MODEL.

Timespan of Simulation	[0, 300]
Number of Time Points	1000
Model Outputs	Q_P, Q_I
Parameters of Interest [Range]	F_T [43.83, 5.57] h [0.36, 0.44] V_b [36.45, 44.55] PS [11.97, 14.63] V_e [26.46, 32.34] σ_1 [0, 0.1] σ_2 [0, 0.1]

B. Predator-Prey (PP) Model

$$[x(0), y(0)] = [0.6, 0.8] \quad (16)$$

$$dx = x \left(a - bx - \frac{cy}{m+x} \right) dt + \alpha x dB_1 \quad (17)$$

$$dy = y \left(r - \frac{fy}{m+x} \right) dt + \beta y dB_2 \quad (18)$$

where x (y) is the prey (predator) population, a is the growth rate of x , b measures the strength of intra-species competition among x , f and c are the maximum values of the per-capita reduction rate of x due to y , m is the environment protection rate of x and y , r is the growth rate of y , α and β are the intensities of the noise processes.

TABLE II
SIMULATION CONDITIONS FOR PREDATOR-PREY (PP) MODEL.

Timespan of Simulation	[0, 100]
Number of Time Points	1000
Model Outputs	x, y
Parameters of Interest [Range]	a [1.8, 2.2], b [0.72, 0.88], c [0.63, 0.77], f [1.44, 1.76] m [1.8, 2.2] r [1.44, 1.76] α [0, 0.1], β [0, 0.1]

C. Convergence Error (CE)

$$CE = \left| \frac{x_{\theta, K}(t) - x_{\theta, K-\delta}(t)}{x_{\theta, K}(t)} \right| \quad (19)$$

where $x_{\theta, K}(t)$ is the interpolated model state at time t with K realizations and parameters θ , and δ is the increment in the number of realizations.

REFERENCES

- [1] S. Ditlevsen and A. Samson, "Introduction to Stochastic Models in Biology," in *Springer-Verlag Berlin Heidelberg*, ser. Lecture Notes in Mathematics, M. Bachar, J. Batzel, and S. Ditlevsen, Eds. Berlin, Heidelberg: Springer Berlin Heidelberg, 2013, vol. 2058, pp. 3–35. [Online]. Available: <http://link.springer.com/10.1007/978-3-642-32157-3> http://link.springer.com/10.1007/978-3-642-32157-3_1
- [2] M. M. Donahue, G. T. Buzzard, and A. E. Rundell, "Experiment design through dynamical characterisation of non-linear systems biology models utilising sparse grids." *IET systems biology*, vol. 4, no. 4, pp. 249–62, jul 2010. [Online]. Available: <http://www.ncbi.nlm.nih.gov/pubmed/20632775>
- [3] J. N. Bazil, G. T. Buzzard, and A. E. Rundell, "A Global Parallel Model based Design of Experiments Method to Minimize Model Output Uncertainty," *Bulletin of mathematical biology*, vol. 74, no. 3, pp. 688–716, mar 2012. [Online]. Available: <http://www.ncbi.nlm.nih.gov/pubmed/21989566>
- [4] T. Mdluli, G. T. Buzzard, and A. E. Rundell, "Efficient Optimization of Stimuli for Model-Based Design of Experiments to Resolve Dynamical Uncertainty," *PLoS Computational Biology*, vol. 11, no. 9, p. e1004488, sep 2015. [Online]. Available: <http://dx.plos.org/10.1371/journal.pcbi.1004488>
- [5] T. Gerstner and M. Griebel, "Dimension-Adaptive Tensor-Product Quadrature," *Computing*, vol. 71, no. 1, pp. 65–87, aug 2003. [Online]. Available: <http://link.springer.com/10.1007/s00607-003-0015-5>
- [6] H.-J. Bungartz and M. Griebel, "Sparse grids," *Acta Numerica*, vol. 13, p. 147, 2004.
- [7] T. Gerstner and M. Griebel, "Sparse grids (Quantitative Finance)," *Encyclopedia of Quantitative Finance*, vol. 13, p. 5, 2008.
- [8] M. Andreucut, "Stochastic recovery of sparse signals from random measurements," *Engineering Letters*, vol. 19, no. 1, pp. 1–6, 2011.
- [9] F. Nobile, R. Tempone, and C. G. Webster, "A Sparse Grid Stochastic Collocation Method for Partial Differential Equations with Random Input Data," *SIAM Journal on Numerical Analysis*, vol. 46, no. 5, pp. 2309–2345, jan 2008. [Online]. Available: <http://epubs.siam.org/doi/abs/10.1137/060663660>
- [10] X. Ma and N. Zabarar, "An Adaptive Hierarchical Sparse Grid Collocation Algorithm for the Solution of Stochastic Differential Equations," *Journal of Computational Physics*, vol. 228, no. 8, pp. 3084–3113, 2009. [Online]. Available: <http://dx.doi.org/10.1016/j.jcp.2009.01.006>
- [11] N. Agarwal and N. R. Aluru, "A Domain Adaptive Stochastic Collocation Approach for Analysis of MEMS under Uncertainties," *Journal of Computational Physics*, vol. 228, no. 20, pp. 7662–7688, 2009. [Online]. Available: <http://dx.doi.org/10.1016/j.jcp.2009.07.014>
- [12] —, "Weighted Smolyak Algorithm for Solution of Stochastic Differential Equations on Non-uniform Probability Measures," *International Journal for Numerical Methods in Engineering*, vol. 85, no. 11, pp. 1365–1389, mar 2011. [Online]. Available: <http://doi.wiley.com/10.1002/nme.3019>
- [13] M. Liu, Z. Gao, and J. S. Hesthaven, "Adaptive Sparse Grid Algorithms with Applications to Electromagnetic Scattering under Uncertainty," *Applied Numerical Mathematics*, vol. 61, no. 1, pp. 24–37, 2011.
- [14] S. Sankaran and A. L. Marsden, "A Stochastic Collocation Method for Uncertainty Quantification and Propagation in Cardiovascular Simulations," *Journal of Biomechanical Engineering*, vol. 133, no. 3, p. 31001, 2011. [Online]. Available: <http://www.scopus.com/inward/record.url?eid=2-s2.0-79956288227&partnerID=tZOTx3y1%5Cnhttp://www.scopus.com/inward/record.url?eid=2-s2.0-79551619583&partnerID=tZOTx3y1%5Cn>
- [15] G. Zhang, M. Gunzburger, and W. Zhao, "A Sparse-Grid Method for Multi-Dimensional Backward Stochastic Differential Equations," *Journal of Computational Mathematics*, vol. 31, no. 3, pp. 221–248, 2013. [Online]. Available: <http://www.global-sci.org/jcm/volumes/v31n3/pdf/313-221.pdf>
- [16] R. Pulch, "Stochastic Collocation and Stochastic Galerkin Methods for Linear Differential Algebraic Equations," *Journal of Computational and Applied Mathematics*, vol. 262, pp. 281–291, 2014. [Online]. Available: <http://dx.doi.org/10.1016/j.cam.2013.10.046>
- [17] Z. Zhang, M. V. Tretyakov, B. Rozovskii, and G. E. Karniadakis, "A Recursive Sparse Grid Collocation Method for Differential Equations with White Noise," *SIAM Journal on Scientific Computing*, vol. 36, no. 4, pp. A1652–A1677, 2014. [Online]. Available: <http://arxiv.org/abs/1310.5605%5Cnhttp://epubs.siam.org/doi/abs/10.1137/130938906>
- [18] S. A. Vavilov and K. Y. Ermolenko, "On the New Stochastic Approach to Control the Investment Portfolio," *IAENG International Journal of Applied Mathematics*, vol. 38, no. 1, pp. 54–62, 2008.
- [19] K. Du, G. Liu, and G. Gu, "Accelerating monte carlo method for pricing multi-asset options under stochastic volatility models," *IAENG International Journal of Applied Mathematics*, vol. 44, no. 2, pp. 62–70, 2014.
- [20] T. Székely and K. Burrage, "Stochastic Simulation in Systems Biology," *Computational and Structural Biotechnology Journal*, vol. 12, no. 20-21, pp. 14–25, nov 2014. [Online]. Available: <http://dx.doi.org/10.1016/j.csbj.2014.10.003> <http://linkinghub.elsevier.com/retrieve/pii/S2001037014000403>
- [21] T. Manninen, M.-L. Linne, and K. Ruohonen, "Developing Itô stochastic differential equation models for neuronal signal transduction pathways," *Computational biology and chemistry*, vol. 30, no. 4, pp. 280–291, 2006.
- [22] A. Saارينen, M.-L. Linne, and O. Yli-Harja, "Modeling Single Neuron Behavior Using Stochastic Differential Equations," *Neurocomputing*, vol. 69, pp. 1091–1096, 2006.
- [23] —, "Stochastic Differential Equation Model for Cerebellar Granule Cell Excitability," *PLoS Computational Biology*, vol. 4, no. 2, p. e1000004, 2008. [Online]. Available: <http://www.pubmedcentral.nih.gov/articlerender.fcgi?artid=2265481&tool=pmcentrez&rendertype=abstract>
- [24] A. K. Duun-Henriksen, S. Schmidt, R. M. Røge, J. B. Møller, K. Nørgaard, J. B. Jørgensen, and H. Madsen, "Model Identification using Stochastic Differential Equation Grey-Box Models in Diabetes," *Journal of diabetes science and technology*, vol. 7, no. 2, pp. 431–440, jan 2013. [Online]. Available: <http://www.pubmedcentral.nih.gov/articlerender.fcgi?artid=3737645&tool=pmcentrez&rendertype=abstract>
- [25] C. Surulescu and N. Surulescu, "Some Classes of Stochastic Differential Equations as an Alternative Modeling Approach to Biomedical Problems," 2013, pp. 269–307. [Online]. Available: http://link.springer.com/10.1007/978-3-319-03080-7_9
- [26] U. Picchini, S. Ditlevsen, and A. De Gaetano, "Modeling the euglycemic hyperinsulinemic clamp by stochastic differential equations," *Journal of Mathematical Biology*, vol. 53, no. 5, pp. 771–796, 2006.
- [27] H. Zhou and M. Liu, "Analysis of a Stochastic Predator-Prey Model in Polluted Environments," *IAENG International Journal of Applied Mathematics*, vol. 46, no. 4, pp. 445–456, 2016.
- [28] A. Klimke and B. Wohlmuth, "Algorithm 847: spinterp: Piecewise Multilinear Hierarchical Sparse Grid Interpolation in MATLAB," *ACM Transactions on Mathematical Software*, vol. 31, no. 4, pp. 561–579, 2005. [Online]. Available: <http://dl.acm.org/citation.cfm?id=1114275>
- [29] T. Gerstner and M. Griebel, "Numerical Integration using Sparse Grids," *Numerical Algorithms*, vol. 18, pp. 209–232, 1998.
- [30] V. Barthelmann, E. Novak, and K. Ritter, "High Dimensional Polynomial Interpolation on Sparse Grids," *Advances in Computational Mathematics*, vol. 12, pp. 273–288, 2000.
- [31] A. Klimke, K. Willner, and B. Wohlmuth, "Uncertainty Modeling using Fuzzy Arithmetic based on Sparse Grids: Applications to Dynamic Systems," *International Journal of Uncertainty, Fuzziness and Knowledge-Based Systems*, vol. 12, no. 6, pp. 745–759, 2004.
- [32] A. Klimke, "Sparse Grid Interpolation Toolbox User's Guide," *IANS report*, 2006.

- [33] D. J. Higham, "An Algorithmic Introduction to Numerical Simulation of Stochastic Differential Equations," *SIAM Review*, vol. 43, no. 3, pp. 525–546, jan 2001. [Online]. Available: <http://dx.doi.org/10.1137/S0036144500378302> <http://epubs.siam.org/doi/abs/10.1137/S0036144500378302>
- [34] T. Sauer, "Numerical Solution of Stochastic Differential Equations in Finance," in *Handbook of Computational Finance*. Berlin, Heidelberg: Springer Berlin Heidelberg, 2012, vol. 47, no. 1, pp. 529–550. [Online]. Available: http://link.springer.com/10.1007/978-3-642-17254-0_19
- [35] —, "Computational Solution of Stochastic Differential Equations," *Wiley Interdisciplinary Reviews: Computational Statistics*, vol. 5, no. 5, pp. 362–371, sep 2013. [Online]. Available: <http://doi.wiley.com/10.1002/wics.1272>
- [36] C. Ji, D. Jiang, and N. Shi, "A Note on a Predator-Prey Model with Modified Leslie-Gower and Holling-type II Schemes with Stochastic Perturbation," *Journal of Mathematical Analysis and Applications*, vol. 377, no. 1, pp. 435–440, 2011. [Online]. Available: <http://dx.doi.org/10.1016/j.jmaa.2009.05.039>